

GaN Photocathodes for UV detection and Imaging

O.H.W. Siegmund^a, A.S. Tremsin^a, A. Martin^a, J. Malloy^a, M. Ulmer^b, B. Wessels^c

^aExperimental Astrophysics Group, Space Sciences Laboratory
University of California at Berkeley, Berkeley CA 94720, USA

^bDepartment of Physics and Astronomy, Northwestern University,
Evanston, IL, 60208-2000, USA

^cDepartment of Materials Science and Engineering, Northwestern University,
Evanston, IL, 60208-3108, USA

ABSTRACT

The nitride-III semiconductors, in particular GaN (band gap energy 3.5 eV), AlN (band gap 6.2 eV) and their alloys $Al_xGa_{1-x}N$ are attractive as UV photo-convertors with applications as photocathodes for position sensitive detector systems. These can "fill the gap" in the 150-400nm wavelength regime between alkali halide photocathodes ($<2000\text{\AA}$), and the various optical photocathodes ($>4000\text{\AA}$, mutlialkali & GaAs). Currently CsTe photocathodes have fairly low efficiency (Fig. 1) in the 100nm to 300nm regime are sensitive to contamination and have no tolerance to gas exposure. We have prepared and measured a number of GaN photocathodes in opaque and semitransparent modes, achieving $>50\%$ quantum efficiency in opaque mode and $\sim 35\%$ in semitransparent mode (Fig. 2). The GaN photocathodes are stable over periods of >1 year and are robust enough to be re-activated many times. The cutoff wavelength is sharp, with a rapid decline in quantum efficiency at $\sim 380\text{-}400\text{nm}$. Application of GaN photocathodes in imaging devices should be feasible in the near future. Further performance improvements are also expected as GaN fabrication and processing techniques are refined.

Keywords: Photocathode, Gallium Nitride, photon counting, Ultraviolet

1. INTRODUCTION

Recent extensive developments in the production of thin layers of GaN type semiconductors for high brightness electron emitters, also make them very promising candidates for visible-blind UV photocathodes which are stable under gas and radiation exposure¹. Benjamin et al², 1996 and others^{3,4} have also reported negative electron affinity for $Al_xGa_{1-x}N$, with $x \sim 0.7\text{-}0.75$. Meanwhile, Machuca et al⁵ 2000 have reported high GaN QE's (50% at 310nm) using Cs activation, and show evidence that activated GaN should be much more robust than GaAs as a stable photoemitter. Early results on "opaque" P (Mg) doped GaN photocathodes [Ulmer et al⁶ 2001, Fig 3] with Cs activation were encouraging. We have re-measured these original sealed tube samples several times and confirmed that there does not seem to be any measurable degradation over several years. Therefore it is possible that GaN based cathodes will be more robust and achieve high ($>50\%$) QDE from the MgF_2 window cutoff to $\sim 400\text{nm}$, where the long wavelength cutoff may be modified (300 – 400nm) by Al or In doping to change the effective bandgap.

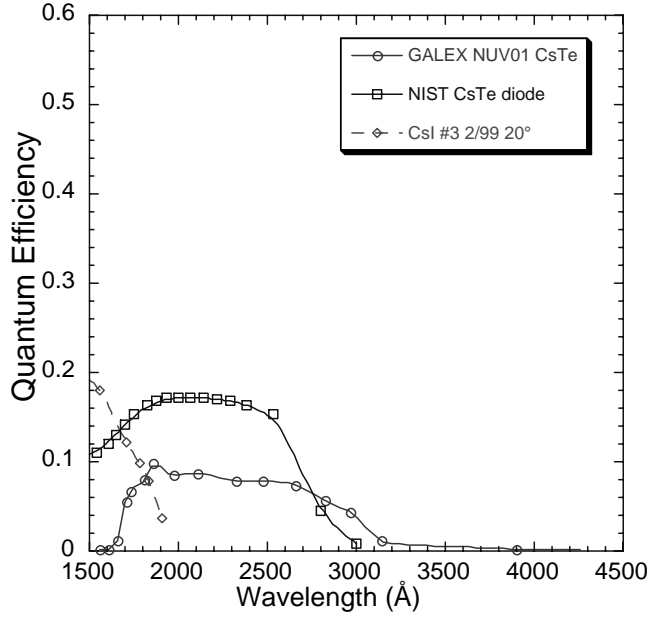


Fig. 1. Measured quantum efficiency of CsI on MCP's, CsTe semitransparent (NIST) on MgF_2 window and CsTe semitransparent (GALEX) on thick UV silica windows.

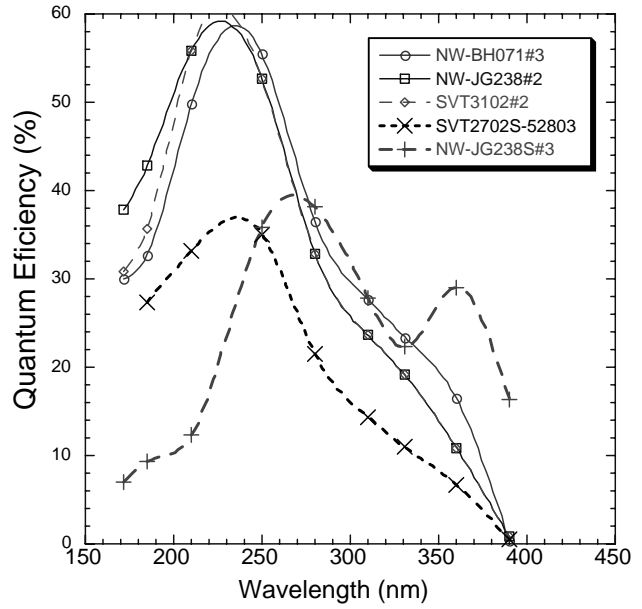


Fig. 2. Measured quantum efficiency of GaN samples on sapphire substrates, in semitransparent (corrected for substrate transmission) and opaque modes.

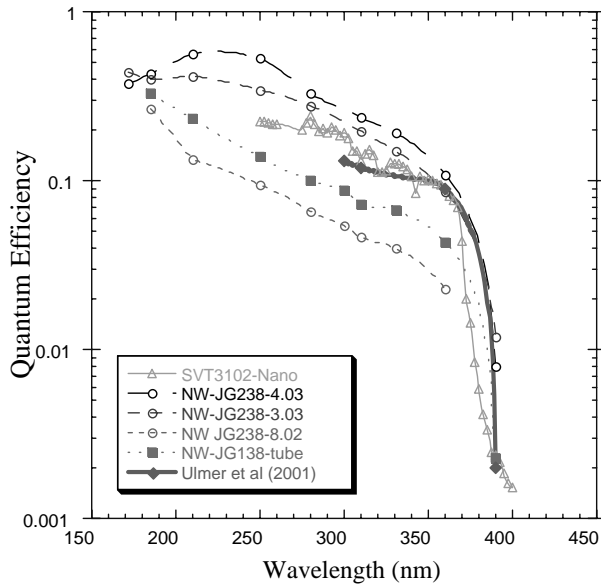


Fig. 3. Measured quantum efficiency of GaN samples on sapphire substrates, opaque mode, showing the evolution of sample processing techniques on the QE.

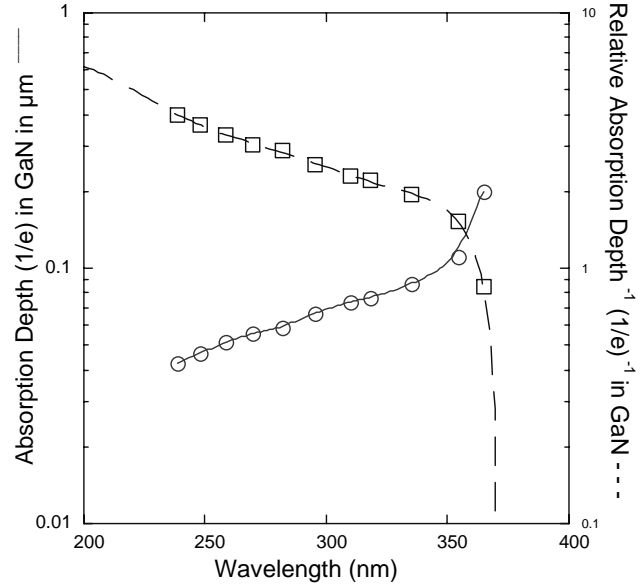


Fig. 4. Calculated $1/e$ attenuation depth for GaN [Muth et al⁷ 1999] and relative $(1/e)^{-1}$ as a function of wavelength, showing the behavior at the band gap.

2.GAN SAMPLES

Given the attenuation characteristics of GaN (Fig. 4), the layers required to absorb UV photons are in the range of 100nm to 1 μm depending on the wavelength. Based on the crystalline structure

of GaN, we have used sapphire for the substrate material as it is a good match for CVD or MBE deposition of GaN films. Our early tests used an Mg doped GaN layer on sapphire from ATMI measured as a “photodiode” without any special activation treatment. As expected the QE was very poor, but not negligible, activation with Cs increased the quantum efficiency considerably however. We have since obtained GaN samples (2” diameter) on sapphire from SVT associates, and additional samples were made at Northwestern University (NWU). The SVT samples have a thin layer of AlN (~100Å) and a 0.1 – 0.15 μm GaN top layer Mg doped (~10¹⁷). The NWU samples are similar except that the GaN layer is ~1 μm thick. The sample data is detailed in Table I.

Table I
Specifications for GaN samples

Sample ID	Thickness	R (ohm.cm)	Hole # cc/cm ³	Mobility cm ² /v.s	Polished Sides
SVT-102112702	0.1um	8.65	7.22E+16	10	two
SVT-102120202	0.15um	>25	--	--	one
SVT-102053102	0.12um	2.96	2.1E+17	26.9	two
NW-BH071	1um	3.64	1.72E+17	10	one
NW-JG219	1um	2.8	2.20E+17	10	one
NW-JG220	1um	2.7	2.30E+17	10	one
NW-JG238	1.1um	2.93	1.83E+17	11.7	one
NW-JG138	1um	7.06	1.01E+17	8.75	one

Ideally, all photons would interact in the GaN layer and electrons created would all drift to the exit surface and be emitted. In practice the attenuation length of photons in GaN⁷ increases with increasing wavelength and increases sharply at the band edge where GaN becomes transparent. To promote electron drift to the layer surface the GaN is Mg (p) doped, and it has been reported⁸ that the minority carrier diffusion length in this material is ~2000Å. The substrate/GaN boundary is prepared with a potential barrier layer to reflect electrons back to the surface⁵, by depositing a thin barrier layer of AlN directly to the substrate. Finally the samples were subjected to stringent chemical and heat cleaning prior to cesiation, which produces the desired negative electron affinity characteristics that promote electron emission. The relative merits of using opaque (front surface illumination and emission) and semitransparent (substrate side illumination and GaN front surface emission) are discussed in a companion paper⁹ in these proceedings. Both scenarios have been evaluated since they each have specific applications, and the combined data gives a better diagnostic of the operation of the cathodes. One issue affecting the GaN efficiency in the semitransparent mode is the substrate transmission. We measured approximately 85% transmission (above 300nm) for the 300μm sapphire substrates with two sides polished and ~75% for the substrates with one side polished.

3.GaN PROCESSING AND MEASUREMENT

Prior to installing the GaN samples into the UHV tank for processing and measurements they were cleaned, first to remove general contaminants and then with a hot acid bath to obtain a very

clean GaN surface. The flat samples were mounted in holders, four of which could be simultaneously mounted inside the UHV tank with electrical signal outputs. These could be attached to an electrometer for measuring the photocurrent. After a general bakeout of the UHV tank to expel water vapor and contaminants, the samples were heat treated ($>600^{\circ}\text{C}$) to degas the surface, followed by a Cs activation process. Just prior to Cs activation we observed $>2\%$ QDE at 254nm from the samples, showing that they are photoemissive even before the NEA treatment. One sample was chosen to monitor the response, then Cs was applied in cycles until the photoresponse was maximized. The same basic process was used to produce a sealed tube (ITT NV) with one of the NWU samples in opaque mode (MgF_2 window).

The absolute QDE values were then measured from narrow band flux measurement comparisons with reference standard NIST calibrated photodiodes. A deuterium hollow cathode light source was used with a set of narrow band interference filters to define a set of measurement wavelengths. The absolute flux was measured with NIST Silicon and CsTe photodiodes, and compared with the photocurrent of the GaN samples. For both measurement configurations (opaque & semitransparent) the tank windows were sapphire. The sapphire window transmission was measured using the same source and NIST diode technique and has been accounted for in these measurements.

4. GaN QUANTUM EFFICIENCY

4.1. GaN quantum efficiency comparisons

It is clear that the quantum efficiency of GaN compares well with the performance of CsTe photocathodes in the same bandpass (Figs. 1 & 2). Indeed the quantum efficiency is significantly higher and has a longer cutoff wavelength (400nm v.s. 300nm) as expected from the GaN properties. The evolution of the data in Fig.2. is detailed in Fig.3. which shows that on a single sample early processing achieved high efficiency at short wavelength, but poor efficiency at the longer wavelengths. Improvement in the processing technique resulted in a small improvement at short wavelengths but almost an order of magnitude improvement at the longer wavelengths. This can be explained as improvements in the effectiveness of the NEA surface activation by cesiation as a result of better cleaning techniques. We conclude that the sealed tube results for a similar sample shows that it was processed in a non-optimal way. To first order the quantum efficiency curve follows the $(1/e)^{-1}$ curve of Fig. 4. which would indicate that the electron escape probability follows an approximately linear dependence on the photon absorption depth. This is not exactly the case, and a more detailed model is discussed in Ulmer et al⁹ 2003 (this conference). However, it is a useful tool in understanding the behavior of the cathode performance.

4.2. GaN quantum efficiency stability

We have re-measured the Ulmer et al⁶ 2001 original sealed tube samples several times and confirmed that there does not seem to be any measurable degradation over several years. We have also performed tests on our activated samples in the UHV chamber. No degradation was observed over periods of months with the chamber at pressures in the low 10^{-9} Torr regime. Deliberate degradation of the vacuum to 10^{-7} Torr for a period of ~ 1 day produced the results shown in Fig. 5. This is interesting in that all samples behave similarly, with a small quantum efficiency loss at short

wavelength and a significantly larger loss with increasing wavelength. Since the bulk transport properties of the GaN should not be changing, the basic interpretation is that the NEA Cs surface layer is being compromised resulting in the greater attenuation of the lower energy photoelectrons produced at longer wavelengths. The sealed tube with sample JG138 was also found to be stable (within measurement limits) over a period of ~ 1 year (Fig. 6. shows data over 6 months). Since this is a UHV vacuum tube and has an internal getter we expect the internal pressure to be quite low (10^{-9} Torr). Another important discovery was that after backfilling the UHV chamber with nitrogen we were able to recover to half the initial GaN QDE by a moderate temperature, high vacuum bake, without re-cesiation, attesting to the robustness of the GaN activation process. The GaN samples have also been repeatedly cleaned and re-activated, as we will discuss below, with consistent results. Thus GaN seems to be a stable and hardy material, although it is clear that the surface activation is a critical issue for GaN

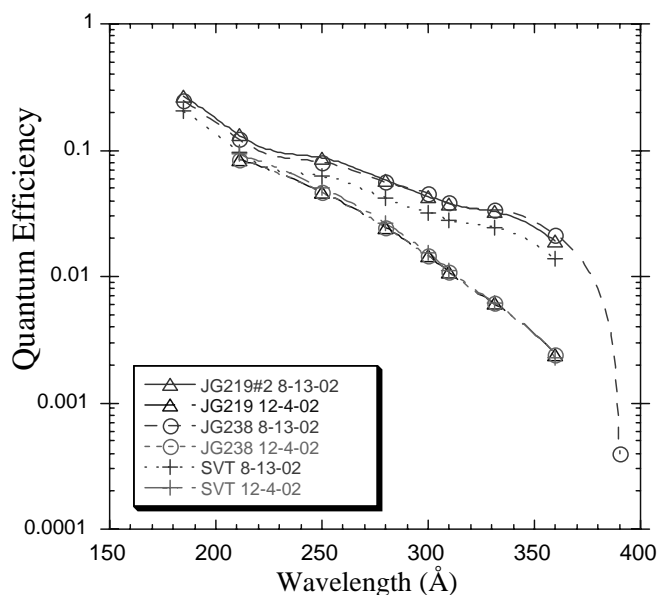


Fig. 5. Measured quantum efficiency of GaN samples on sapphire substrates, opaque mode, showing the QE degradation after exposure to 10^{-7} torr conditions.

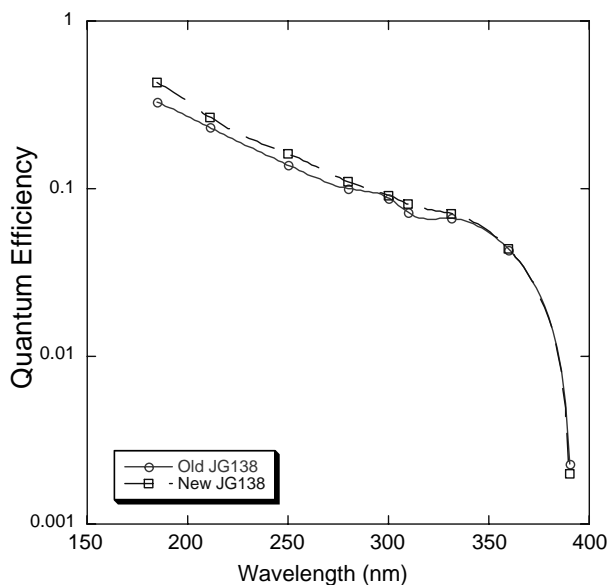


Fig. 6. Measured quantum efficiency of a sealed tube opaque GaN sample over a period of 6 months. There is no measurable degradation within error margins.

4.3. Opaque GaN quantum efficiency

Several of the SVT and NWU samples were processed and tested as opaque photocathodes. They were also tested as semitransparent cathodes, however for the purposes of the Cs activation the sensing and control of the activation was always done using one of the samples in opaque mode. Figs. 7 and 8 show the opaque GaN quantum efficiency for two SVT and one NWU sample all in the same pumpdown and activation batch, that were Cs activated on two separate occasions. Between the Cs activations a high temperature ($>500^{\circ}\text{C}$) bake of the samples was performed to release the surface Cs from the prior activation. The NWU JG220 sample achieves $>40\%$ quantum efficiency peak and gives almost identical results for both Cs activations. This is also the case for the SVT2702 sample, except that $>30\%$ quantum efficiency peak is reached. For a similar sample process run the SVT3102 and NWU BH071 and JG238 samples (Fig. 9, 10) showed much better

(>50% quantum efficiency) but the best depends on the activation run and the sample used for the activation control. As a process control a sample of the SVT3102 wafer was sent to Nanosciences Inc and was prepared and activated there by a similar, but not identical procedure. The results are presented in Fig. 9 and show a slightly lower quantum efficiency, but a similar wavelength dependence, except for the cutoff. Their more detailed spectrometer measurements at the band edge better define the rapidity and extent of the GaN quantum efficiency dropoff compared to our narrow band filter measurements. Clearly there is a well defined dropoff at about 370nm that decays by two orders of magnitude over ~40nm.

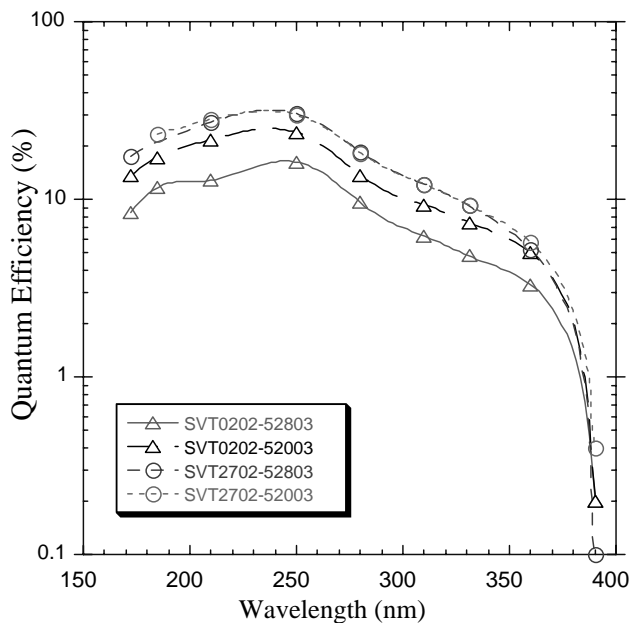


Fig.7. Measured quantum efficiency of SVT GaN samples on sapphire substrates, opaque mode, showing the QE for two samples after two independent cesiations.

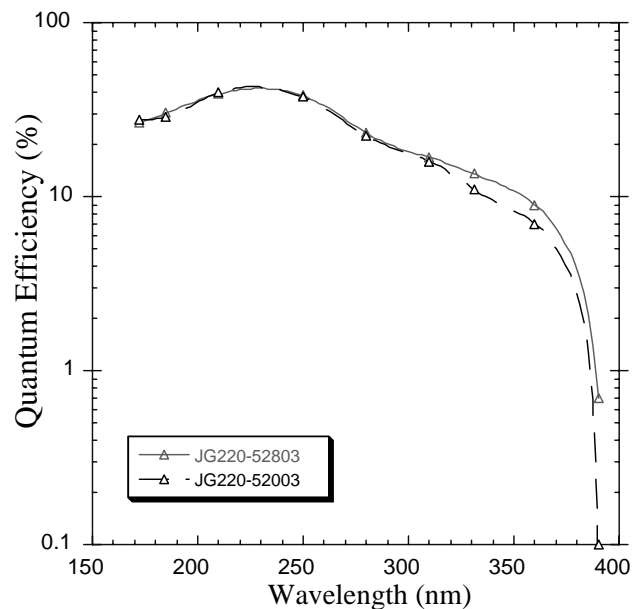


Fig.8. Measured quantum efficiency of NWU GaN sample on sapphire substrate, opaque mode, showing the QE after two independent cesiations.

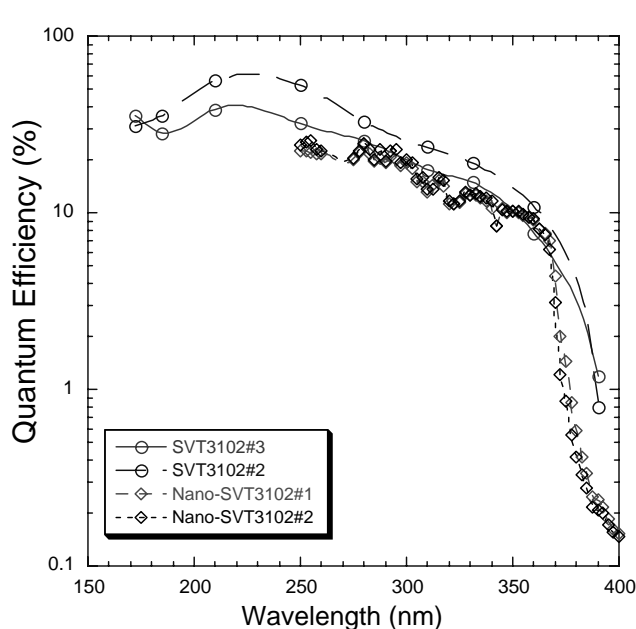


Fig.9. Measured quantum efficiency of SVT GaN wafer samples on sapphire substrate, opaque mode, showing the QE after two independent cesiations each. cesiations.

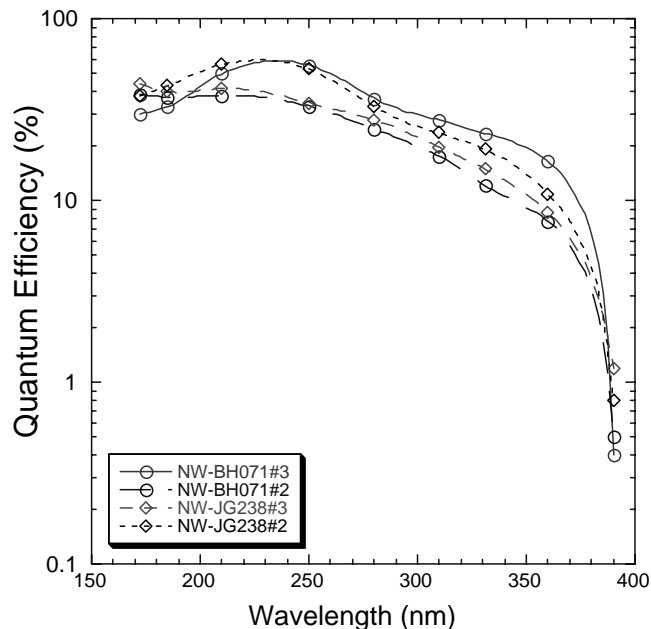


Fig.10. Measured quantum efficiency of NWU GaN on sapphire substrates, opaque mode, showing the QE for two samples after two independent

It is also interesting that the thin ($0.1\mu\text{m}$ layer – SVT) and thick ($1\mu\text{m}$ layer NWU) GaN give very similar results, suggesting that photons interacting deeper than 100nm do not play a great role in the quantum efficiency. It is also interesting though that the last Cs activation of BH071 produced a significantly higher red response, and lower blue response than before. The poor performance of the SVT0202 samples is probably due to the poor sample resistivity and most likely low dopant level with consequently poor mobility values. The SVT2702 is also comparatively not as good as SVT3102 for the same reasons. So as suggested by Ulmer et al 2003 (these proceedings) the conductivity and mobility are important to achieve high quantum efficiency. It is not clear why NWU JG220 is not as good as the other samples, but we find this also to be true for its semitransparent performance that is discussed below. One other feature that seems consistent in all the data is a dropoff in quantum efficiency below 200nm . This feature will be confirmed by future measurements with MgF_2 windows down to 110nm , but a quantum efficiency drop at $\sim 200\text{nm}$ would be expected since at $2x$ the bandgap energy we expect the onset of double photoelectron production with low kinetic energy. This would be very similar to our observations of quantum efficiency in alkali halide photocathodes¹⁰.

4.4. Semitransparent GaN quantum efficiency

The UHV vacuum tank was configured with sapphire windows either side of the samples so that they could also be tested as semitransparent cathodes. The SVT 2702 and 0202 samples were activated twice with similar results (Fig. 11). The 0202 sample is worse than the 2702 sample again presumably due to the bulk material properties as described above. However, the uncorrected efficiency of the SVT 2702 sample is quite high (30%) indicating a good electron escape probability. The NWU JG220 sample (Fig. 12) produced very poor semitransparent quantum

efficiency – far worse than its opaque performance and that of any other sample in semitransparent mode. It is not clear why this is so, but it seems to indicate that there is some layer between the sapphire and GaN that may be strongly affecting the transmission of photons. The SVT 3102 and NWU BH071 and JG238 samples were processed in an earlier run, and their semitransparent efficiency is shown in Figs. 13 and 14. In all cases the efficiency of the third Cs activation produced the best efficiency results. This may be due to the fact that this earlier run had a less optimized cleaning procedure and several processes were needed to achieve the cleanliness required. The SVT has reasonable efficiency (~20%) and the NWU samples are up to 30% quantum efficiency. Such high efficiencies for the thick NWU samples show that the electrons must be able to be transported from close to the substrate-GaN interface up to the emission surface. Also the Cs activation of the surface is more critical for the semitransparent mode than the opaque mode.

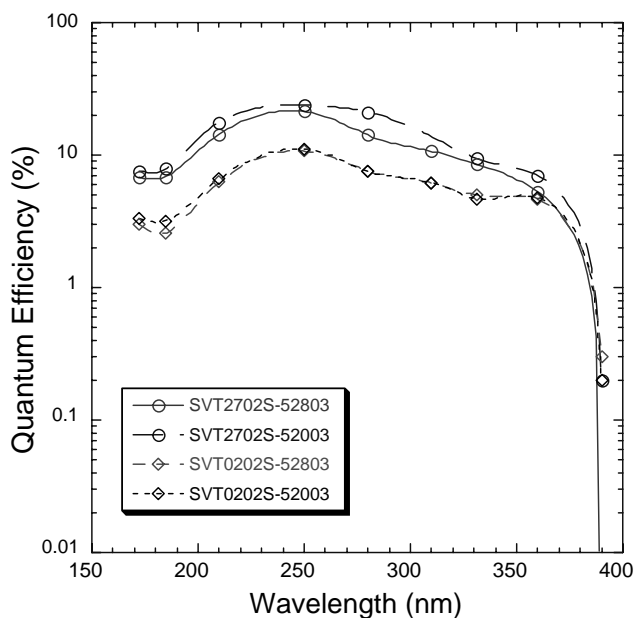


Fig.11. Measured quantum efficiency of two SVT GaN samples on sapphire, semitransparent mode, showing the QE after two cesiations. Not corrected for substrate transmission.

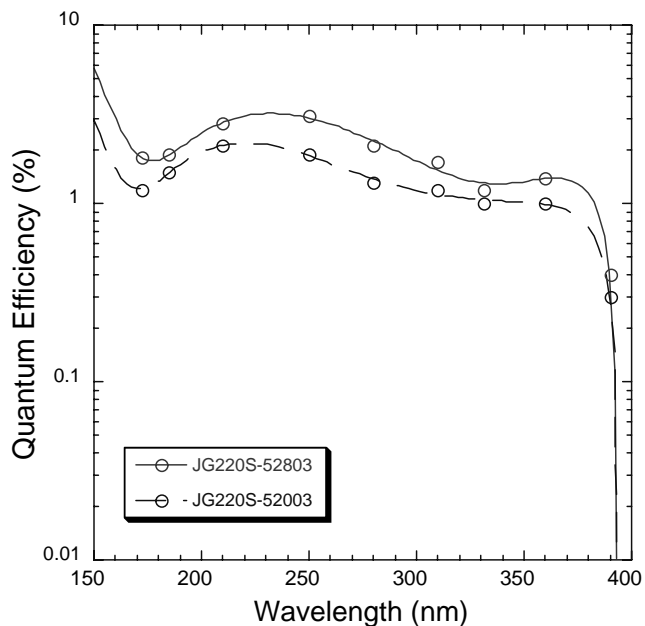


Fig.12. Measured quantum efficiency of NWU GaN on sapphire, semitransparent mode, showing the QE after two cesiations. Not corrected for substrate transmission.

As shown in Fig. 2. there is a marked difference between the thin and thick GaN cathodes in semitransparent mode. For the thin cathodes the blue wavelengths are absorbed in the thin layer and the photoelectrons escape into vacuum, but the red wavelengths are mostly transmitted (Fig. 4), so the response is blue peaked. In the case of the thick GaN samples the blue wavelengths are absorbed close to the substrate – GaN layer boundary producing photoelectrons, but these do not escape the cathode vacuum surface side. Red wavelengths interacting closer to the vacuum interface do produce electrons that escape. Therefore there is a short wavelength dropoff in the thick sample data and the red response is generally better.

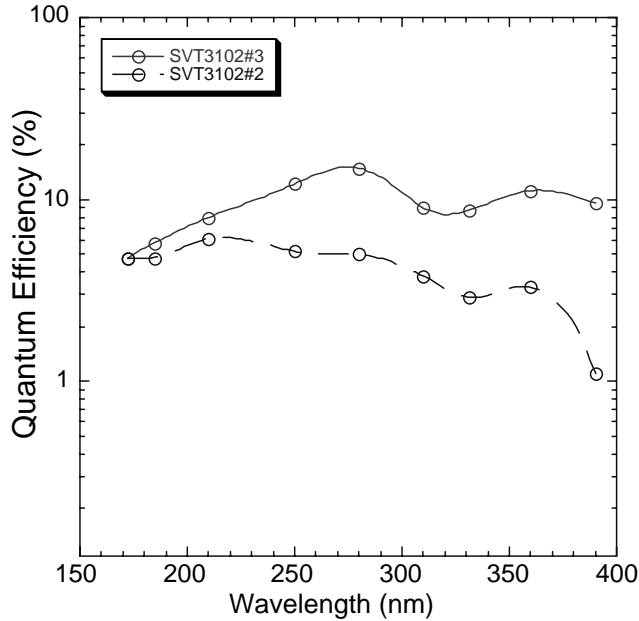


Fig.13. Measured quantum efficiency of a SVT GaN sample on sapphire, semitransparent mode, showing the QE after two cesiations. Not corrected for substrate transmission.

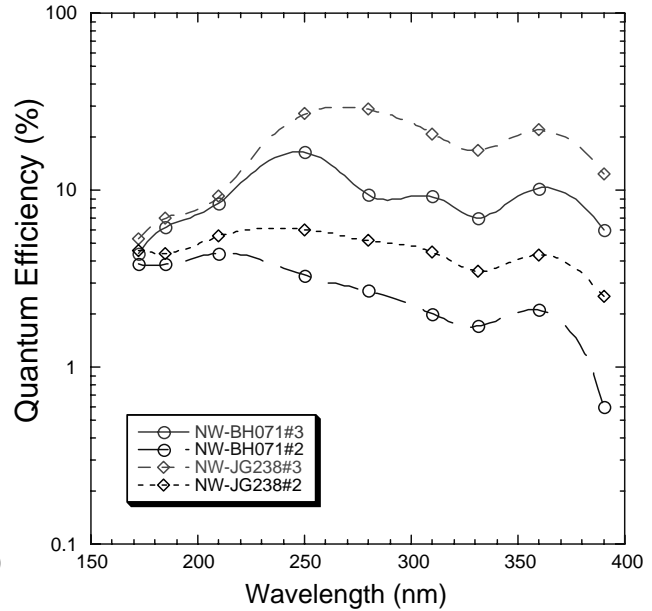


Fig.14. Measured QE of two NWU GaN samples on sapphire, semitransparent mode, showing the QE after two cesiations. Not corrected for substrate transmission.

5.GaN PROSPECTS

The quantum efficiency and stability of GaN photocathode layers is much higher than the currently available cathode technology (CsTe). There is room for considerable optimization of the materials and processing techniques that should allow high efficiency performance over a broad band (100nm – 400nm). An increase in the carrier concentration to improve the conductivity and mobility of the bulk GaN layer seems likely to help the quantum efficiency. In addition improvements in GaN cleaning and Cs activation will probably help improve the red response. Even at this stage the increases in quantum efficiency over CsTe imply that future astronomical applications will obtain significant enhancement. Both GALEX and STIS instruments are a factor of more than three lower in QE than even the semitransparent GaN samples tested here. Implementation of opaque GaN is also potentially feasible if layers can be deposited on Silicon MCP's¹¹ as polycrystalline layers (BH071 is half polycrystalline).

Based on current results GaN semitransparent photocathodes deposited on sapphire windows up to 2" are feasible. The advantage of GaN on sapphire windows is that they can be used as the entrance window of a sealed tube. The cathodes can then be coupled to an imaging 2D detector via a hot indium seal, and a getter enclosed inside the detector for longevity. We have developed imaging tubes of this kind¹² and envisage employing a GaN cathode in the near future.

ACKNOWLEDGEMENTS

This work was supported by NASA grants NAG5-6730, NAG5-8667 NAG5-9149, NAG5-11547 & NAG5-12710. The authors would like to thank Joel Gregie and Bing Han at NWU for fabrication of the GaN samples, nanosciences for processing and measurement of GaN samples, and John Vallerga and Patrick Jelinsky at UCB for participating in the measurements.

REFERENCES

1. Monroy, E., F. Calle, C. Angulo, P. Vila, A. Sanz, J. A. Garrido, E. Calleja, E. Muñoz, S. Haffouz, B. Beaumont, F. Omnes, and P. Gibart, *Applied Optics*, Volume 37, Issue 22, pp.5058-5062 (1998)
2. Benjamin, M.C.; Bremser, M.D. et al., *App. Surf. Sci.*, 104, 455 (1996)
3. Nemanich RJ, Baumann PK, Benjamin MC, Nam OH, Sowers AT, Ward BL, Ade H, Davis RF, *Applied Surface Science* 132: pp.694-703 (1998)
4. Hatfield, C. W. and G. L. Bilbro, *Journal of Vacuum Science & Technology B: Microelectronics and Nanometer Structures*, Volume 17, Issue 5, pp.1987-1992, (1999)
5. Machuca, F., Y. Sun, Z. Liu, K. Ioakeimidi, P. Pianetta, and R. F. W. Pease, *Journal of Vacuum Science & Technology B: Microelectronics and Nanometer Structures*, Volume 18, Issue 6, pp.3042-3046, (2000)
6. Ulmer, M. P., B. W. Wessels, F. Shahedipour, R. Y. Korotkov, C. L. Joseph, and T. Nihashi, *Proc. SPIE Vol. 4288*, p. 246-253 (2001)
7. J. F. Muth, J. D. Brown, M. A. L. Johnson, Zhonghai Yu, R. M. Kolbas, J. W. Cook, Jr. and J. F. Schetzina, Absorption coefficient and refractive index of GaN, AlN and AlGaN alloys, *J. Nitride Semicond. Res.* 4S1, G5. 1999.
8. Bandic, Z. Z., P. M. Bridger, E. C. Piquette, and T. C. McGill, *Applied Physics Letters*, Volume 73, Issue 22, pp.3276-3278 (1998)
9. M. P. Ulmer, B. W. Wessels, B. Han, J. Gregie, A. Tremsin, and O. H. W. Siegmund, "Advances in Wide-Band-Gap Semiconductor Based Photocathode Devices for Low Light Level Applications, these proceedings.
10. O. H. W. Siegmund Advances in microchannel plate detectors for UV/visible Astronomy, *Proc. SPIE Vol. 4854*, pp 181-190, 2002
11. O. H. W. Siegmund, A. S. Tremsin, C. P. Beetz, Jr., R. W. Boerstler, D. R. Winn, "Progress on development of silicon microchannel plates", *SPIE Proc.*, vol. 4497, 139-148, 2001
12. P. Jelinsky, P. Morrissey, J. Malloy, S. Jelinsky, and O. Siegmund, C. Martin, D. Schiminovich, K. Forster, T. Wyder and P. Friedman, Performance Results of the GALEX cross delay line detectors, *Proc. SPIE Vol. 4854*, pp 233-240, 2002.